Published in final edited form as:
Biochemistry. 2006 August 29; 45(34): 10260–10269. doi:10.1021/bi060490t.

CFTR Expression in Human Neutrophils and the Phagolysosomal Chlorination Defect in Cystic Fibrosis

Richard G. Painter[1], **Vincent G. Valentine**[2], **Nicholas A. Lanson Jr.**[1], **Kevin Leidal**[3], **Qiang Zhang**[4], **Gisele Lombard**[2], **Connie Thompson**[2], **Anand Viswanathan**[1], **William M. Nauseef**[3], **Guangdi Wang**[4], and **Guoshun Wang**[1,*]

[1] Departments of Medicine and Genetics, Gene Therapy Program, Louisiana State University Health Sciences Center, New Orleans, LA 70112, USA

[2] Lung Transplantation Program, Ochsner Clinic Foundation, New Orleans, LA 70121, USA

[3] The Inflammation Program, Department of Medicine, The University of Iowa, and the Veterans Affairs Medical Center, Iowa City, IA, 52242

[4] Department of Chemistry, Xavier University of Louisiana, New Orleans, LA 70125, USA

Abstract

Production of hypochlorous acid (HOCl) in neutrophils, a critical oxidant involved in bacterial killing, requires chloride anions. Because the primary defect of cystic fibrosis (CF) is the loss of chloride transport function of the CF transmembrane conductance regulator (CFTR), we hypothesized that CF neutrophils may be deficient in chlorination of bacterial components due to limited chloride supply to the phagolysosomal compartment. Multiple approaches, including RT-PCR, immunofluorescence staining, and immunoblotting, were used to demonstrate that CFTR is expressed in resting neutrophils at the mRNA and protein levels. Probing fractions of resting neutrophils isolated by Percoll gradient fractionation and free flow electrophoresis for CFTR revealed its presence exclusively in secretory vesicles. The CFTR chloride channel was also detected in phagolysosomes, a special organelle formed after phagocytosis. Interestingly, HL-60 cells, a human promyelocytic leukemia cell line, upregulated CFTR when induced to differentiate into neutrophils with DMSO, strongly suggesting its potential role in mature neutrophil function. Analyses by gas chromatography and mass spectrometry (GC/MS) revealed that neutrophils from CF patients had a defect in their ability to chlorinate bacterial proteins from *Pseudomonas aeruginosa* metabolically pre-labeled with ^{13}C-L-tyrosine, unveiling defective intraphagolysosomal HOCl production. In contrast, both normal and CF neutrophils exhibited normal extracellular production of HOCl when stimulated with phorbol ester, indicating that CF neutrophils had the normal ability to produce this oxidant in the extracellular medium. This report provides the evidence to suggest that CFTR channel expression in neutrophils and its dysfunction affects neutrophil chlorination of phagocytosed bacteria.

Cystic fibrosis (CF), the most common genetic disease in caucasians, is caused by mutations of the gene encoding the CF transmembrane conductance regulator (CFTR), a cAMP-regulated chloride channel (1,2). CF has long been recognized as an epithelial disease whose most severe complications often occur in the lung. The clinical manifestations include persistent bacterial infection, prominent neutrophil infiltration and small airway obstruction (3). Despite dramatic

Correspondence: Guoshun Wang, D.V.M., Ph.D., 642 CSRB, 533 Bolivar St., Louisiana State University Health Sciences Center, New Orleans, LA 70112, Phone: (504) 568-7908, Fax: (504) 568-8500, gwang@lsuhsc.edu.

advances in our understanding of the molecular and cellular basis of CF, there remains a paradox of why the mobilized neutrophils fail to eradicate bacterial infections in the lung.

Neutrophils are professional phagocytes, responsible for elimination of pathogens and cell debris. During phagocytosis, neutrophils demonstrate a dramatic increase in metabolic activities including a burst of oxygen consumption and increased turnover by the hexose monophosphate shunt (4,5). Nicotinamide adenine dinucleotide phosphate-dependent (NADPH) oxidase was first found to be responsible for the respiratory burst (6), which leads to the production of superoxide free radicals (7). Superoxide is then dismutated to hydrogen peroxide (H_2O_2). Subsequently, myeloperoxidase (MPO), present predominantly in neutrophils, catalyzes the reaction of H_2O_2, H^+, and chloride (Cl^-) to generate hypochlorous acid (HOCl) as follows:

$$Cl^- + H_2O_2 + H^+ \xrightarrow{MPO} HOCl + H_2O$$

Chloride is considered the major physiological halide involved in this reaction. Even though superoxide radicals can mediate direct killing of ingested bacteria, considerable evidence indicates that HOCl and hydrogen peroxide play major roles in bacteria killing (8–10). Of these two oxidants, HOCl is by far the most toxic and broad spectrum, presumably due to its broad chemical reactivity with bacterial proteins, lipids and nucleic acids (9,10). Moreover, bacterial killing by neutrophils is blocked by inhibition of phagocyotsis, indicating that the killing process is mostly confined to the phagolysosomal compartment (11).

Here we report that CFTR is expressed in neutrophils and neutrophils from CF patients are impaired in chlorination of ingested bacteria due to defective hypochlorous acid (HOCl) production within phagolysosomes, which may potentially limit their ability to kill susceptible bacteria. Interestingly, extracellular HOCl production by CF neutrophils is normal, indicating their competency in generating this oxidant. Defective intraphagolysosomal and competent extracellular HOCl production by CF neutrophils is consistent with the loss of Cl^- transport function of CFTR within the phagolysosomes.

MATERIALS AND METHODS

Chemicals

Percoll was obtained from BD Pharmacia (San Diego, CA). Glybenclamide (GBA), salicylhydroxamic acid (SHA), human male AB serum, saponin, *Aspergillus niger* catalase, taurine, diethylenetriaminepentaacetic acid (DEPA) and other common chemicals were obtained from Sigma (St Louis, MO). $Na^{125}I$ and L-[U-^{14}C] amino acid mixture were obtained from Amersham Biosciences (Piscataway, NJ). *Pseudomonas aeruginosa* was obtained from Dr. Michael Schurr at Tulane University Health Sciences Center (New Orleans, LA).

Isolations of neutrophils and PAO1-containing phagolysosomes

Human peripheral blood neutrophils were isolated using the Percoll method previously described (12). In all cases, endotoxin-free reagents and plastic ware were used to avoid activating the cells. The human subject protocol was approved by the IRBs of Louisiana State University Health Sciences Center at New Orleans and Ochsner Clinic Foundation. Yields of $4–6 \times 10^7$ neutrophils were typically obtained from 18–20 ml of blood. Phagolysosomes were prepared from neutrophils that had been allowed to ingest opsonized PAO1 at a ratio of 1:10 (PMN:PAO1) for 15–30 min using a modified procedure published previously (13). Briefly, neutrophils were pre-treated with the membrane permeable serine protease inhibitor diisopropryl fluorophosphate (DFP, Sigma). After incubation with bacteria, the neutrophil-

bacteria complexes were washed from free bacteria with ice-cold medium by centrifugation at 150× *g* for 5 min at 4° C. The neutrophil pellets containing ingested PAO1 were resuspended in 250 mM sucrose containing 3 mM imidazole (pH 7.4) and a cocktail of protease inhibitors (Sigma). The neutrophils were lysed by repeatedly passing through a 23-gauge needle. After a low speed centrifugation at 300× *g* for 5 min to remove intact cells and nuclei, the supernatant was layered onto a 12% sucrose cushion containing 3 mM imidazole (pH 7.4) and centrifuged at 800× *g* for 45 min at 4°C. The pellet fraction which contained phagolysosomes was resuspended in a solution of 250 mM sucrose with 3 mM imidazole buffer and immediately used for immunofluorescent staining.

Immunofluorescent localization of CFTR

CFTR was localized using the following two antibodies: 1) mouse monoclonal CFTR antibody 24.1 directed against a C-terminal cytoplasmic epitope (R & D System, Minneapolis, MN), and 2) affinity-purified rabbit polyclonal CFTR antibody against an N-terminal peptide corresponding to amino acids 1–182 of CFTR (Santa Cruz Biotech, Santa Cruz, CA). The antibody against lysosome-associated membrane protein-1 (LAMP-1) was obtained from the Developmental Studies Hybridoma Bank (Iowa, IA). For immunostaining of intact neutrophils, Percoll-purified cells were allowed to settle and adhere to glass coverslips for 10 min at 37° C. For some experiments, as indicated, serum-opsonized GFP-PAO1 bacteria were added and phagocytosis allowed to proceed for 5–30 min. Otherwise, the cells were directly fixed with 2% paraformaldehyde for 30 min at room temperature and then washed twice with Tris-buffered saline (TBS). The cells were permeabilized with 0.5% saponin in TBS containing a protease inhibitor cocktail (Sigma) for 10 min and then blocked with 2% normal goat serum in TBS containing the protease inhibitors for 1 hour. Primary antibody (CFTR-24.1) was added at the dilution of 1:50 and incubated for 1 hour at room temperature. After 5 washes with TBS, the coverslips were then counterstained with Alexa-568 goat anti-mouse IgG (1:500) for 1 hour. After 5 ten-minute washes with TBS, the cells were post-fixed with 2% paraformaldehyde for 10 min and then washed twice with PBS. The coverslips were mounted on microscopic slides with Vectasheild (Vector Laboratories, Burlingame, CA) containing DAPI which stains nuclei. Images were obtained by confocal microscopy. When double labeling with CFTR and LAMP-1 was desired, non-fluorescent PAO1 were used instead of GFP-PAO1. The isolated PAO1-laden phagolysosomes were similarly stained for CFTR and LAMP-1 after allowing the purified phagolysosomes to settle and adhere to polybrene-coated coverslips in the presence of 2% paraformaldehyde/PBS buffer (pH 7.2). The CFTR and LAMP-1 primary antibodies were diluted to 1:50, and the secondary antibodies Alexa-568 goat anti-mouse IgG and Alexa-488 goat anti-rabbit IgG (Molecular Probes, Eugene, OR) were used at a dilution of 1:500. Preliminary control experiments indicated that PAO1 alone did not stain with the above reagents and protocols.

Reverse transcription-PCR

Total RNAs were prepared by the Trizol reagent (Invitrogen, Carsbad, CA). As previously published (14), the human CFTRWT reverse primer (5′-CATCATAGGAAACA-CCAAA-3′) and the TATA box-binding protein (TBP) reverse primer (5′-ATTGGACTAAAGA-TAGGGA-3′)were used together in one reaction to reverse-transcribe their mRNAs to their corresponding cDNAs using the thermoscript RT-PCR system (Invitrogen). The primers for PCR amplification of CFTR were human CFTRWT forward primer (5′-GGATTTGGGGAAT-TATTTGAGAAAG-3′)and the human CFTRWT reverse primer described above. The primers for PCR amplification of TBP were the TBP forward primer(5′-CGTGTGAAGATAA-CCCAAG-3′) and the TBP reverse primer described above. The CFTR PCR program was as follows:1 cycle at 95°C for 3 min; 41 cycles (30 sec at 95°C, 30 sec at 44°C, and 60 sec at 74° C), and then a final extension step at 74°C for 20 min. The TBP PCR-amplification condition was identical except annealing temperature was 49°C for 38 cycles.

HL-60 differentiation by DMSO and immunoblot analysis

HL-60 cells were originally obtained from ATCC. For dimethyl sulfoxide (DMSO)-induced differentiation, HL60 cells were started at an initial density of 2×10^5 cells/ml in the RPMI 1640 medium supplemented with 1.25% DMSO (Sigma Chemical Co., St. Louis, MO). Sequential samples were collected on days 1–4, respectively. On day three, the medium was replenished by centrifuging the cells out and replating in the same volume of fresh medium containing 1.25% DMSO.

For Western blots, HL-60 cells or purified human neutrophils were treated with 10% trichloroacetic acid (TCA) in DPBS for 1 hour at 4°C. The use of TCA is critical in rapidly inactivating neutrophil proteases to prevent CFTR degradation. Next, the samples were centrifuged at 4 °C for 15 min on a microfuge and the pellets washed three times in cold 100% ethanol. The pellets were air-dried at room temperature and dissolved in sample buffer (62.5 mM Tris pH 6.8, 1.5% SDS, 5% glycerol, 1× Sigma protease inhibitor cocktail). Samples were briefly sonicated to facilitate solubilization of the protein pellet. The protein concentration was quantified using a Bio-Rad protein assay kit. The samples were diluted to a concentration of 1 μg/μl, and 30 μg were applied per lane. The proteins were separated on 7.5% SDS-polyacrylamide gels and transferred onto nitrocellulose membranes. The membranes were blocked for 1 hour in TBS-T containing 5% dried milk and 1% goat serum. The primary antibody (CFTR 24-1, R & D Systems) was used at a 1:600 dilution. The secondary antibody (Bio-Rad GAM-HRP) was diluted to 1:2500 for use. After extensive washes, the proteins were visualized using the Pierce ECL kit (Pierce, Rockford, IL) per the manufacturer's procedure. Amersham Hyperfilm-ECL was exposed for 10 minutes to overnight.

Isolation and characterization of neutrophil subcellular fractions

Neutrophil subcellular fractions were isolated according to previous publications (8,15,16, 42). Briefly, isolated PMNs ($1,200\times10^6$) were pretreated with DFP and cavitated in 2 ml of 1× relaxation buffer (100 mM KCl, 3 mM NaCl, 1 mM ATP, 3.5 mM $MgCl_2$, 1.25 mM EGTA, 10 mM piperazine *N*,*N*′-bis2[ethan-sulfonic acid], pH 7.2). The mixture was then centrifuged on a double-layer Percoll gradient (1.05 g/ml and 1.12 g/ml). After centrifugation at 37,000×*g* for 30 minutes at 4°C, three bands were identifiable: Bands α, β and γ. The α-band largely is composed of azurophilic granules with MPO. The β-band contains specific and gelatinase granules. The γ-band contains secretory vesicles and plasma membranes. To further purify secretory vesicles from plasma membranes, we treated the γ fraction with neuraminidase (0.2 units/ml) followed by free flow electrophoresis (FFE) as previously described (17). The conductance of the media buffer or chamber buffer (6 mM triethanolamine, 6 mM acetic acid, 270 mM sucrose, pH 7.4) was adjusted to 0.42 $m\Omega^{-1}$. The electrode buffer is composed of 50 mM triethanolamine, 50 mM acetic acid at a pH of 7.4. The flow rate was set to 3.12 ml per hour per fraction and the current at 100 mA. The alkaline phosphatase activity and the latent alkaline phosphatase activities of each fraction were measured (18). For measurement of latent alkaline phosphatase, 0.2% of Triton X-100 was added to release the latent enzyme. According to the enzyme activity data, fractions for secretory vesicles and plasma membranes were pooled, respectively.

Phagocytosis of $^{13}C_9$-tyrosine labeled PAO1 by neutrophils

GFP-PAO1 bacteria were metabolically labeled with $^{13}C_9$-L-tyrosine by growing for 18–19 hrs in 0.5 ml LB medium containing 1mM of the stable isotope. ^{14}C-labeled amino acids (2.5 μCi; Amersham) were added to monitor recoveries and measure phagocytosis of bacteria by PMN. The labeled bacteria were washed with PBS three times by centrifugation to remove free isotopes, opsonized with human serum, and then washed twice with Cl^--free Ringer's BSS (119 mM sodium gluconate, 1.2 mM magnesium gluconate, 4 mM calcium gluconate, 2.4 mM K_2HPO_4, 0.6 mM KH_2PO_4, 10 mM dextrose, 20 mM HEPES, pH 7.4). To remove bacterial

aggregates the bacteria were passed through a 25-gauge needle three times and centrifuged at 250× *g* for 5 min. The supernatant was harvested. The bacterial density and radioactive isotope incorporation determined by spectrophotometry and liquid scintillation counting, respectively. The labeled GFP-PAO1 (1.25×10^8) were mixed with PMN preincubated at 37° C (1×10^7 per ml) in the Cl^--rich Ringer's BSS containing 10% human serum which had been extensively dialyzed against the Cl^--free BSS. In the phagocytosis mixture, 15 mM taurine and 10 μg/ml bovine catalase were added to suppress chlorination of extracellular bacteria without affecting chlorination of intracellular bacteria (19). Inhibitors, when present, were preincubated with PMN for 10 min prior to the addition of bacteria. After a 1-hour incubation at 37° C with tumbling, the reaction was stopped by the addition of the MPO inhibitor salicylhydroxamic acid (SHA, 200 μM) to block further chlorination. The cells containing phagocytosed bacteria were harvested at 80× *g* and washed three times with cold Cl^--free BSS containing 15 mM taurine, 200 μM SHA and 100 μM diethylenetriaminepentaacetic acid (DEPA) to remove free bacteria. The cell pellet was resuspended in 0.2 ml of water containing 100 μM DEPA, and stored frozen at −80°C until further analysis. Under these conditions approximately 50% of the added bacteria were recovered in the cell pellet.

GC/MS analysis of chlorotyrosine

Samples from above were thawed and delipidated by extraction of the aqueous phase three times with 200 μl of ice-cold chloroform:methanol (2:1 v/v) (19–21). The 3-[ring-$^{13}C_6$]-tyrosine ($^{13}C_6$-Cl-Y; 50 nmol) and 3-[ring-$^{13}C_6$]-chlorotyrosine ($^{13}C_9$-Cl-Y; 20 pmol) were added as the internal standards, followed by lyophilization. The residue was resuspended in 400 μl water. Then, 0.15 ml of 1.0 mg/ml bacterial protease Type XIV (Sigma) was added. The protease solution was prepared in 100 mM Tris/HCl buffer (pH 8.0) containing 10 mM $CaCl_2$. Fresh enzyme was added every 24 hours to ensure a complete protein hydrolysis. After 72 hours of digestion the samples were lyophilized and the aromatic amino acids isolated using a C18 column (Alltech, Deerfield, IL) as described (14). The amino acids were converted to their N(O)-ethoxycarbonyltrifluoroethyl esters by reaction with trifluoroethanol and ethyl chloroformate in pyridine-water as described by Husek (22) and extracted into 150 μl of chloroform containing 2% ethyl chloroformate. The various isotopomers of 3-chloro-L-tyrosine and L-tyrosine present in the samples were measured as described (21). An Agilent 6890N gas chromatography and a 5973N mass selective detector (Agilent Technologies, Palo Alto, CA) equipped with a general purpose HP-5MS capillary column were used for the quantification of 3-chloro-L-tyrosine and L-tyrosine. Briefly, 1 μl of the chloroform extract was injected into the GC/MS using an automatic injector. Bacterial-derived $^{13}C_9$-chlorotyrosine concentrations were calculated from the observed ion-current ratios for m/z 289.1/286.1 ($^{13}C_9$-Cl-Y/$^{13}C_6$-Cl-Y) measured using the selected ion-monitoring mode. Bacterial-derived $^{13}C_9$-L-tyrosine was calculated from the ratio of ions at m/z 327.1/324.1 ($^{13}C_9$-Y/$^{13}C_6$-Y) in a similar fashion. The other specific ion-peaks for chlorotyrosine and tyrosine, reported previously using the identical derivatization method (21), were also detected. We chose the m/z 289.1/286.1 and 327.1/324.1 pairs to determine the chlorotyrosine and tyrosine concentrations because of their high abundance displayed under our experimental conditions. The bacterial-derived 3-chlorotyrosine content of the original samples is expressed as moles per 1000 moles of bacterial-derived tyrosine.

Phagolysosomal iodination assays

GFP-PAO1 bacteria were radiolabeled by growing the cells overnight with shaking in LB medium containing 20–40 μCi per ml of ^{14}C-amino acid mixture. Next, the cells were washed intensively to remove the unincorporated isotope and opsonized with human male AB serum that had been extensively dialyzed against the Cl^--free Ringer's BSS. The ^{14}C-labeled bacteria were phagocytosed by Percoll-purified neutrophils at a ratio of 40 bacteria per neutrophil for 15 min in the Cl^--free Ringer's BSS containing 10% of the dialyzed human AB serum.

Phagocytosis was stopped by adding the ice-cold buffer and washing twice at 200× *g* for 2 min to remove free bacteria. The pellets (1×10^7 cells per tube), resuspended in 100 μl of the pre-warmed buffer containing no serum, were mixed with $Na^{125}I$ (10 μCi). Included in the system was 80 nM KI as a carrier as well as *Aspergillus niger* catalase (10 μg/ml) and 300 μM taurine to trap extracellular H_2O_2. After incubation at 37° C for 15 min to allow $^{125}I^-$ uptake and iodination of the internalized bacteria, 5 volumes of the ice-cold buffer was added and the cells isolated by centrifugation, followed by washes to remove free $^{125}I^-$. The cell pellets, resuspended in 30% glycerol containing 200 μg/ml of lysozyme and 5 μl of the Sigma protease inhibitor cocktail, were lysed by adding 0.2 volumes of 5× immunoprecipitation buffer (250 mM Tris/Cl, pH 7.2, 750 mM NaCl, 5% Triton X-100, 0.5% sodium deoxycholate, 0.1% SDS). After 15 min on ice, pre-washed Pansorbin A (Calbiochem, La Jolla, CA) was added and incubated for 15 min and then centrifuged at 14000× *g* at 4° C. The cleared supernatants were harvested and either rabbit polyclonal anti-GFP antibody (Molecular Probes, Eugene, OR) or normal rabbit serum as a specificity control was added. After a two-hour incubation on ice, protein A/G Sepharose (Santa Cruz Biotech) was added and the samples gently rocked for 1 hour at 4° C. The samples were then centrifuged at 14000× *g* at 4° C for 1 min and the Protein A/G Sepharose pellets washed 4 times. ^{14}C and ^{125}I levels in the contents were determined by liquid scintillation counting.

Extracellular taurine chlorination

Assays for the chlorination of taurine by MPO were performed according to the published procedure (23). MPO release was induced by treating neutrophils with 500 ng/ml PMA.

RESULTS

Expression of CFTR in human neutrophils and their phagolysosomes

To examine whether CFTR is expressed in human neutrophils, immunofluorescent localization studies were first performed using antibodies specific to CFTR. Confocal microscopy demonstrated that CFTR is present in resting neutrophils in association with intracellular punctate structures (Fig. 1a–b), while no staining was observed using an isotype control antibody (Fig. 1c–d). Surprisingly, no obvious cell surface membrane staining for CFTR was noted. The granule-like staining pattern led us to speculate that CFTR might be localized on neutrophil granule membranes. Thus, we performed double-immunofluorescent staining of normal neutrophils using antibodies against MPO and CFTR (Fig. 1e–h). By direct visualization, MPO stainings were more intense than that of CFTR. Even though some overlapping of the two stainings was observed, the two proteins were not fully co-localized (Fig. 1h). The numbers of strongly stained punctate structures and limited resolution of the microscopic method precluded an accurate judgment of co-expression of the two proteins in the azurophilic granules where abundant MPO is known to be stored (15). Nevertheless, it is clear that the majority of CFTR was associated with membrane-bounded intracellular structures. It is well-known that during phagocytosis neutrophil granules and other intracellular membrane-bound structures (i.e. secretory vesicles) fuse with phagosomes to form phagolysosomes (24). During this process, granule and vesicle contents are discharged into this organelle, initiating bacterial killing, while their membrane proteins become part of the phagolysosomal membranes. Therefore, we predicted that the membrane-associated CFTR would be found in the membranes of phagolysosomes. To assess the prediction, we fed normal neutrophils serum-opsonized *Pseudomonas aeruginosa* which expressed the green fluorescent protein (GFP-PAO1). Immuofluorescent staining revealed the association of CFTR with the phagocytosed GFP-PAO1 (Fig. 1i–l, large arrows) or structures resembling phagocytic vacuoles (Fig. 1i–l, arrowheads). Bacteria alone similarly fixed and permeabilized did not show any detectable staining for CFTR (data not shown). Because the confocal micrographs are cross-sectional images, the rod-like GFP-PAO1 appeared to be round. Early granule-

phagosome attachment prior to the membrane fusion stage was also observed (Fig. 1i–l, small arrows). To further confirm this finding, we biochemically isolated phagolysosomes from homogenates of neutrophils which had ingested non-fluorescent PAO1. Bacteria in the isolated phagolysosomes were demonstrated by DAPI staining (Fig. 1m) using fluorescent microscopy. The rod-like PAO1 bacteria were clearly shown. Antibodies directed against lysosome-associated membrane protein-1 (LAMP-1) (Fig. 1n) and CFTR (Fig. 1o) showed a clear co-localization of the two proteins on the membranes of the PAO1-bearing phagolysosomes (Fig. 1p). A free PAO1 (Fig. 1m–p, arrows) in the preparation did not show any CFTR or LAMP-1 staining, indicating the specificity of the antibodies. Since LAMP-1 is only found in the membranes of late phagolysosomes, but not cytoplasmic or early phagosome membranes (25), we conclude that CFTR was expressed in the membrane of phagolysosomes formed after phagocytosis.

To evaluate CFTR mRNA presence in human neutrophils, we did reverse transcription-PCR (RT-PCR) analyses of total neutrophil RNAs. Two CFTR-specific primers were used with the forward primer on exon 9 and the reverse one on exon 10, as described in our previous publication (14). The intron between the two exons is 10,640 bp. This design allows the amplification of the reverse-transcribed cDNA, but not the amplification of contaminating genomic DNA that might be present. As a control, we performed a separate RT-PCR using a pair of primers for TATA-box binding protein (TBP), a ubiquitously expressed protein. As shown in Fig. 2a, human neutrophils express CFTR at the mRNA level as the positive control of Calu-3 cells, an airway submucosal gland epithelial cell line which is known to abundantly express CFTR.

To validate the CFTR protein expression in neutrophils, we performed Western blot analyses on total neutrophil and differentiated HL-60 cell proteins. A total of 30 μg of protein for each sample was resolved in a 7.5% SDS-polyacrylamide gel, followed by immunoblotting using the CFTR-specific antibody. Three immunoreactive bands from the CFTR-gene-corrected CF airway epithelial cells were apparent albeit with varied expression levels (Fig. 2b). Band A (~130 kDa) is the newly-synthesized non-glycosylated form of CFTR, while Band B (~150 kDa) is the ER core-glycosylated form and Band C (~180–190 kDa) is the fully-glycosylated mature form (26). Human neutrophils had an intense band at the Band C position, suggesting the major form of CFTR in neutrophils is the mature and fully glycosylated one. HL-60 cells are a well-characterized human promyelocytic leukemia cell line. After induction with polar organic compounds such as dimethyl sulfoxide (DMSO), these cells are known to differentiate into neutrophils over a period of 3–6 days (27). After the induction with DMSO, CFTR expression is upregulated in two major forms: Bands A and C. The upregulation peaked at ~Day 3 after DMSO treatment. CFTR expression is enhanced in HL-60 cells with the induction of differentiation to neutrophils, strongly suggesting a potential role for CFTR in mature neutrophil function.

To define the CFTR-positive subcellular structure(s), we isolated subcellular fractions of neutrophils including α, β, plasma membranes and secretory vesicles, as described in Materials and Methods. The α-fraction contains primary or azurophilic granules, while the β-fraction largely consists of specific and gelatinase granules (15). Immunoblotting using the CFTR-specific antibody displayed that CFTR was present primarily in the secretory vesicles (Fig. 2C). It is known that proteins in secretory vesicles are synthesized at a much late stage of myeloid differentiation (15). This result is consistent with the late expression pattern of CFTR in HL-60 cells after DMSO induction.

Defect of CF neutrophils in halogenation of ingested PAO1

We next examined the ability of CF and normal neutrophils to chlorinate PAO1-derived tyrosine residues within the phagolysosome. As illustrated in Figure 3a, neutrophils from

normal or CF donors were first fed serum-opsonized PAO1 which had been metabolically labeled with $^{13}C_9$-L-tyrosine in the presence of catalase and taurine. Catalase and taurine were included to suppress extracellular, but not intracellular, chlorination. One hour after ingestion, free bacteria were removed by repeated low speed centrifugation. The PMN cell pellets, containing ingested bacteria, were delipidated and subjected to protease hydrolysis (20). The levels of PAO-derived ($^{13}C_9$-derived) chlorotyrosine and tyrosine were determined by gas chromatography and mass spectrometry (GC/MS) using the isotope dilution method (21). Because neutrophil-derived tyrosine contains no $^{13}C_9$-L-tyrosine or its derivatives, this is a direct measure of the chlorination of intracellular PAO1-derived tyrosine. Shown in Figure 3b are typical GC/MS elution profiles for $^{13}C_9$-3-chlorotyrosine-specific ions produced from PAO1 which were phagocytosed by CF and normal neutrophils. Figure 3c shows the ratios of PAO1-derived $^{13}C_9$-3-chlorotyrosine produced per 1000 moles of PAO1-derived $^{13}C_9$-tyrosine. Neutrophils from the normal individuals gave a ratio of 1.61 ± 0.38, a value in agreement with previous reports of bacterial chlorination by normal neutrophils (19, 28). However, neutrophils from CF donors had a ratio of 0.35 ± 0.23, which is significantly lower than the normal ($P<0.05$, N=4). Because the bacteria were labeled with ^{14}C-radioactive amino acids, we also measured phagocytotic uptake by measuring TCA-precipitable ^{14}C radioactivity in the same samples used for GC/MS analyses. Normal neutrophils phagocytosed 8.4 +/− 2.3 PAO1 per cell (n=4) compared to 8.8 +/− 1.6 PAO1 per cell (n=5) for CF neutrophils. This result indicates that the difference in bacterial protein chlorination between normal and CF neutrophils is not due to differences in phagocytosis. To determine the factor(s) leading to defective HOCl production in CF neutrophil phagolysosomes, we performed MPO-mediated chlorination of extracellular taurine, which was stimulated by phorbol-12-myristate-13-acetate (PMA). PMA induces the secretion of MPO to the extracellular space. As shown in Figure 3d, CF neutrophils were not impaired in their ability to produce extracellular HOCl compared with normal neutrophils, proving that the levels of active MPO and H_2O_2 produced by CF and normal neutrophils are comparable. This result is in agreement with previous studies showing that CF neutrophils have either no differences or slightly increases, in MPO levels and hydrogen peroxide production (29–31). We, therefore, conclude that a deficiency in the availability of chloride anion to the lumen of the phagolysosome is the most likely explanation for the low levels of intraphagolysosomal chlorination in CF neutrophils.

To further validate the chlorination results above, we performed phagolysosomal iodination assays using radioactive $^{125}I^-$, a totally different strategy from the GC/MS approach. It is well-known that MPO, in the presence of H_2O_2, also has the ability to oxidize bromide (Br^-) and iodide (I^-), generating the corresponding hypohalous acids (7,32,33). Moreover, CFTR has the ability to transport other halides such as bromide and iodide (34–37). As diagramed (Fig. 4a), normal and CF neutrophils were first fed serum-opsonized GFP-PAO1 bacteria that were metabolically pre-labeled with ^{14}C-amino acids. After removal of the free bacteria, the cells were incubated in $^{125}I^-$-containing medium, followed by washes to remove the free $^{125}I^-$. Then, the cells were lysed and the bacterial GFP immunoprecipitated. Specific radioactivity for ^{125}I and ^{14}C in this bacterial protein were measured. The data demonstrated that CF neutrophils iodinated this bacterial protein only ~25% as well as their normal counterparts (Fig. 4b, N=4, $P<0.05$). In contrast, the ^{14}C-GFP counts from both groups were similar, suggesting an equal phagocytosis of bacteria in the two experimental groups (Fig. 4b). Additional experiments compared the rate of uptake of $^{125}I^-$ into the cytoplasm by normal and CF neutrophils. The results showed that normal neutrophils had an uptake of 228.4 ± 23.9 dpm per microgram cellular protein (N=7), and CF neutrophils 196.7 ± 24.8 dpm per microgram cellular protein (N=3), revealing no statistically significant difference. Therefore, the lower rate of iodination of GFP seen in Figure 4b cannot be explained by a reduced uptake of $^{125}I^-$ from the medium into the cytoplasm. Thus, the impaired iodination of bacterial proteins was most likely due to the defective iodide transport from the cytoplasm into the phagolysosomes of CF neutrophils. If so, we would predict that treatment of normal neutrophils with

glybenclamide (GBA), a CFTR-channel blocker, should recapitulate the phenomenon observed in CF neutrophils. To test this, normal neutrophils, after ingestion of ^{14}C-labeled GFP-PAO1 as before, were treated with 200 μM GBA prior to and throughout the exposure of the cells to $^{125}I^-$. After cell lysis, immunoprecipitation of the bacterial GFPs was performed. Measurement of ^{125}I and ^{14}C incorporated in GFP showed that the GBA treatment significantly decreased the iodination level of ^{14}C-GFP to ~60% of that seen in the controls (Fig. 4c, N=5, $P<0.05$). To ensure that the phagolysosomal iodination resulted from the MPO-H_2O_2-halide reaction, we included a group of controls that were treated with 100 μM salicylhydroxamic acid (SHA), an inhibitor of MPO. Under these conditions, radioiodination of ^{14}C-GFP was abolished (Fig. 4c), indicating that the iodination of GFP was MPO-dependent. SHA had no appreciable effect on H_2O_2 release by scopolitin assay or on phagocytosis by ^{14}C-labeled bacterial uptake (data not shown). From these results, we conclude that CFTR present on neutrophil phagolysosomes was functionally involved in transporting halides into this organelle. Because of this, CF neutrophils had an impaired halide secretion into phagolysosomes, thus limiting halogenation of the ingested organisms.

DISCUSSION

In this report, we have demonstrated that human neutrophils and DMSO-treated HL-60 cells express CFTR. The CFTR protein is co-localized to phagolysosomes and exclusively present in isolated secretory vesicles. Importantly, neutrophils from CF patients are defective in chlorination of phagocytosed bacterial proteins, while their extracellular chlorination capacity is normal. These results suggest that CFTR dysfunction may affect chloride supply to phagolysosomes which limits the chlorination reaction in this organelle.

CFTR expression and function in epithelial cells are well studied (38–40). However, CFTR expression in non-epithelial cells such as neutrophils remains poorly defined. There was one study reported that CFTR mRNA transcripts were detected in various non-epithelial cells including freshly isolated neutrophils (41). To our best knowledge, no studies have been reported on CFTR protein presence in human neutrophils. Our immunofluorescent localization data (Fig. 1) as well as the subcellular fractionation data (Fig. 2C) suggest that the cytoplasmic membrane surface appears relatively devoid of CFTR. Thus, phagolysosomal CFTR must come from the vesicles and/or granules which fuse with phagosomal membranes. The immunoblot data support an association of CFTR with secretory vesicles. However, due to the intrinsic instability of the CFTR protein and the high proteolysis probability in neutrophil granules even under stern proteinase inhibition conditions, negative results of CFTR presence in other subfractions should be interpreted with caution. Interestingly, another chloride channel ClC-3 was recently reported to be in the secretory vesicles and secondary granules of resting neutrophils (42). When phagocytosis occurs, the ClC-3 channel was up-regulated to the phagolysosomal membranes. Based on the similarity of their subcellular distributions of CFTR and ClC-3 chloride channels, we predict that the two may have synergistic functions in transport chloride from the cytosol to the phagolysosomal lumens.

According to the MPO-catalyzed chemical reaction, HOCl production is determined by the following four factors: 1) Cl^- availability, 2) MPO level, 3) H_2O_2 level, and 4) H^+ level. In CF neutrophils, the MPO level and H_2O_2 production are normal or higher than that seen in normal neutrophils (29–31). Furthermore, massive H^+ production in phagolysosomes is coupled with superoxide production by phagocyte NADPH oxidase (7–10). Because CF neutrophil H_2O_2 production is normal, the H^+ production should be normal. Therefore, chloride availability is most likely the rate-limiting factor for HOCl production. There are three hypothetical pathways for phagolysosomes to obtain Cl^-: 1) carry-in directly during phagocytosis from the extracellular space, 2) transport from the cytosol through Cl^- channels including CFTR and other Cl^- channels such as ClC3, and 3) Cl^- stored in granules and vesicles

which later fuse with phagosomes after phagocytosis. In our recent publication (43), we found that neutrophils, in a Ringer's buffer containing the physiological level of Cl^-, had an intraphagolysosomal Cl^- level of ~73 mM. However, when neutrophils were placed in a chloride-free isoosmotic medium, the intraphagolysosomal Cl^- level was ~6.6 mM. Under this chloride-free condition, carry-in of Cl^- directly through phagocytosis from the extracellular space was low. Furthermore, due to Cl^- efflux the cytosolic Cl^- level was also low. Therefore, if the granules or vesicles contained a large amount of Cl^-, we should be able to detect a significant level of phagolysosomal Cl^-. The fact that a low level of Cl^- in phagolysosomes was detected under conditions of low extracellular chloride, leads us to conclude that Cl^- generated from granules and/or vesicles by fusion contributes little to intraphagolysosomal Cl^- supply. In this report, we demonstrated that neutrophils from CF patients are defective in intraphagolysosomal HOCl production. In contrast, CF neutrophils are competent in generating HOCl extracellularly, if stimulated to discharge MPO to the extracellular space. These data support our hypothesis that the CFTR Cl^- channel dysfunction may primarily limit Cl^- supply to the phagolysosomes, which affects HOCl production in the organelle. We are aware that ion transports are typically coupled. Abnormal influx or efflux of one ion affects the membrane potential and the ion distribution surrounding the membrane, thus affecting the transport of other ions through channels or pumps. It did not escape our attention that the CFTR channel dysfunction in CF neutrophils may affect H^+ transport to, or retention in, phagolysosomes, even though its production through respiratory burst is normal in CF neutrophils. Future studies are warranted to evaluate the secondary effects of CFTR dysfunction in the overall process.

It is well documented that CF has defective epithelial Cl^- transport. This defect in the lung epithelium results in alterations in the ion composition and in the viscosity of the apical surface fluid in the lung (44). This facilitates bacterial colonization and biofilm formation, blunts the bactericidal capacity of epithelial antimicrobial agents, and affects sputum clearance (45,46). This report documents neutrophil chlorination defect in CF, which when combined with epithelial dysfunction may result in an increasing propensity to the infection of the lungs by opportunistic bacteria. This would explain well why CF, but not MPO-deficient, patients succumb to severe lung infections. Therefore, CF is not only an epithelial disease, but also a neutrophil disease. As a result, correction of both neutrophil CFTR function and epithelial CFTR function may be necessary to obtain maximum therapeutic effects for CF.

Acknowledgments

We thank Sharon Halton for her help with venipunctures. This work would not have been possible without contributions of tissues by the CF patients and normal donors, to whom we are greatly indebted. The authors would like to thank Drs. Paul McCray and Mike Welsh at the University of Iowa for their helpful comments on the experiments. This work was partially supported by Cystic Fibrosis Foundation Research Grant WANG05G0 (to G.W.), NIH AI 34879 (to W.M.N.) and Louisiana Gene Therapy Consortium.

ABBREVIATIONS

PMN	polymorphonuclear neutrophils
NADPH	nicotinamide adenine dinucleotide phosphate, oxidized form
MPO	myeloperoxidase
HOCl	hypochlorous acid
H_2O_2	hydrogen peroxide
PAO1	*Pseudomonas aeruginosa*
CF	cystic fibrosis
CFTR	cystic fibrosis transmembrane conductance regulator

DAPI	4′,6-diamidino-2-phenylindole
GFP	green fluorescent protein
LAMP-1	lysosome-associated membrane protein-1
GC/MS	gas chromatography/mass spectrometry
PMA	phorbol-12-myristate-13-acetate
GBA	glybenclamide
SHA	salicylhydroxamic acid
DMSO	dimethyl sulfoxide
TBP	TATA box binding protein
RT-PCR	Reverse transcription polymerase chain reaction

References

1. Rommens JM, Iannuzzi MC, Kerem B, Drumm ML, Melmer G, Dean M, Rozmahel R, Cole JL, Kennedy D, Hidaka N, et al. Identification of the cystic fibrosis gene: chromosome walking and jumping. Science 1989;245:1059–1065. [PubMed: 2772657]
2. Riordan JR, Rommens JM, Kerem B, Alon N, Rozmahel R, Grzelczak Z, Zielenski J, Lok S, Plavsic N, Chou JL, et al. Identification of the cystic fibrosis gene: cloning and characterization of complementary DNA. Science 1989;245:1066–1073. [PubMed: 2475911]
3. Welsh, MJ.; Ramsey, BW.; Accurso, F.; Cutting, G. Cystic Fibrosis. In: Scriver, CR., editor. Metabolic and Molecular Basis of Interited Disease. New York: McGraw-Hill; 2001. p. 5121-5188.
4. Baldridge C, Gerard R. The extra respiration of phagocytosis. Am J Physiol 1933;103:235–236.
5. Sbarra AJ, Karnovsky ML. The biochemical basis of phagocytosis. I. Metabolic changes during the ingestion of particles by polymorphonuclear leukocytes. J Biol Chem 1959;234:1355–1362. [PubMed: 13654378]
6. Rossi F, Zatti M. Biochemical aspects of phagocytosis in polymorphonuclear leucocytes. NADH and NADPH oxidation by the granules of resting and phagocytizing cells. Experientia 1964;20:21–23. [PubMed: 4379032]
7. Klebanoff SJ. Myeloperoxidase: friend and foe. J Leukoc Biol 2005;77:598–625. [PubMed: 15689384]
8. DeLeo FR, Allen LA, Apicella M, Nauseef WM. NADPH oxidase activation and assembly during phagocytosis. J Immunol 1999;163:6732–6740. [PubMed: 10586071]
9. Foote CS, Goyne TE, Lehrer RI. Assessment of chlorination by human neutrophils. Nature 1983;301:715–716. [PubMed: 6828155]
10. Albrich JM, McCarthy CA, Hurst JK. Biological reactivity of hypochlorous acid: implications for microbicidal mechanisms of leukocyte myeloperoxidase. Proc Natl Acad Sci U S A 1981;78:210–214. [PubMed: 6264434]
11. Okuda K. Effects of cytochalasin B on the intrcellular bactericidal activity of human neutrophils. Antimicrob Agents Chemother 1975;7:736–741. [PubMed: 1155917]
12. Lindena J, Burkhardt H. Separation and chemiluminescence properties of human, canine and rat polymorphonuclear cells. J Immunol Methods 1988;115:141–147. [PubMed: 2848071]
13. Perskvist N, Roberg K, Kulyte A, Stendahl O. Rab5a GTPase regulates fusion between pathogen-containing phagosomes and cytoplasmic organelles in human neutrophils. J Cell Sci 2002;115:1321–1330. [PubMed: 11884531]
14. Wang G, Bunnell BA, Painter RG, Quiniones BC, Tom S, Lanson NA Jr, Spees JL, Bertucci D, Peister A, Weiss DJ, et al. Adult stem cells from bone marrow stroma differentiate into airway epithelial cells: potential therapy for cystic fibrosis. Proc Natl Acad Sci U S A 2005;102:186–191. [PubMed: 15615854]

15. Borregaard N, Cowland JB. Granules of the human neutrophilic polymorphonuclear leukocyte. Blood 1997;89:3503–21. [PubMed: 9160655]
16. Kjeldsen L, Sengelov H, Borregaard N. Subcellular fractionation of human neutrophils on Percoll density gradients. J Immunol Methods 1999;232:131–143. [PubMed: 10618515]
17. Sengelov H, Nielsen MH, Borregaard N. Separation of human neutrophil plasma membrane from intracellular vesicles containing alkaline phosphatase and NADPH oxidase activity by free flow electrophoresis. J Biol Chem 1992;267:14912–7. [PubMed: 1634531]
18. Kjeldsen L, Sengelov H, Lollike K, Borregaard N. Granules and secretory vesicles in human neonatal neutrophils. Pediatr Res 1996;40:120–129. [PubMed: 8798257]
19. Chapman AL, Hampton MB, Senthilmohan R, Winterbourn CC, Kettle AJ. Chlorination of bacterial and neutrophil proteins during phagocytosis and killing of Staphylococcus aureus. J Biol Chem 2002;277:9757–9762. [PubMed: 11733505]
20. Pietzsch J. Measurement of 5-hydroxy-2-aminovaleric acid as a specific marker of iron-mediated oxidation of proline and arginine side-chain residues of low-density lipoprotein apolipoprotein B-100. Biochem Biophys Res Commun 2000;270:852–857. [PubMed: 10772915]
21. Pietzsch J, Kopprasch S, Bergmann R. Analysis of 3-chlorotyrosine as a specific marker of protein oxidation: the use of N(O,S)-ethoxycarbonyltrifluoroethyl ester derivatives and gas chromatography/mass spectrometry. Rapid Commun Mass Spectrom 2003;17:767–770. [PubMed: 12672128]
22. Husek P. Amino acid derivatization and analysis in five minutes. FEBS Lett 1991;280:354–356. [PubMed: 2013337]
23. Kettle AJ, Winterbourn CC. Assays for the chlorination activity of myeloperoxidase. Methods Enzymol 1994;233:502–512. [PubMed: 8015486]
24. Zucker-Franklin D, Hirsch JG. Electron Microscope Studies on the Degranulation of Rabbit Peritoneal Leukocytes During Phagocytosis. J Exp Med 1964;120:569–576. [PubMed: 14212120]
25. Bainton DF. Distinct granule populations in human neutrophils and lysosomal organelles identified by immuno-electron microscopy. J Immunol Methods 1999;232:153–168. [PubMed: 10618517]
26. Farinha CM, Mendes F, Roxo-Rosa M, Penque D, Amaral MD. A comparison of 14 antibodies for the biochemical detection of the cystic fibrosis transmembrane conductance regulator protein. Mol Cell Probes 2004;18:235–242. [PubMed: 15271383]
27. Collins SJ, Ruscetti FW, Gallagher RE, Gallo RC. Terminal differentiation of human promyelocytic leukemia cells induced by dimethyl sulfoxide and other polar compounds. Proc Natl Acad Sci U S A 1978;75:2458–2462. [PubMed: 276884]
28. Rosen H, Crowley JR, Heinecke JW. Human neutrophils use the myeloperoxidase-hydrogen peroxide-chloride system to chlorinate but not nitrate bacterial proteins during phagocytosis. J Biol Chem 2002;277:30463–30468. [PubMed: 12060654]
29. Brockbank S, Downey D, Elborn JS, Ennis M. Effect of cystic fibrosis exacerbations on neutrophil function. Int Immunopharmacol 2005;5:601–608. [PubMed: 15683855]
30. Koller DY, Urbanek R, Gotz M. Increased degranulation of eosinophil and neutrophil granulocytes in cystic fibrosis. Am J Respir Crit Care Med 1995;152:629–633. [PubMed: 7633718]
31. Van Der Vliet A, Nguyen MN, Shigenaga MK, Eiserich JP, Marelich GP, Cross CE. Myeloperoxidase and protein oxidation in cystic fibrosis. Am J Physiol Lung Cell Mol Physiol 2000;279:L537–546. [PubMed: 10956629]
32. Gaut JP, Yeh GC, Tran HD, Byun J, Henderson JP, Richter GM, Brennan ML, Lusis AJ, Belaaouaj A, Hotchkiss RS, Heinecke JW. Neutrophils employ the myeloperoxidase system to generate antimicrobial brominating and chlorinating oxidants during sepsis. Proc Natl Acad Sci U S A 2001;98:11961–11966. [PubMed: 11593004]
33. Henderson JP, Byun J, Williams MV, Mueller DM, McCormick ML, Heinecke JW. Production of brominating intermediates by myeloperoxidase. A transhalogenation pathway for generating mutagenic nucleobases during inflammation. J Biol Chem 2001;276:7867–7875. [PubMed: 11096071]
34. Simchowitz L. Interactions of bromide, iodide, and fluoride with the pathways of chloride transport and diffusion in human neutrophils. J Gen Physiol 1988;91:835–860. [PubMed: 3047312]
35. Schultz BD, Singh AK, Devor DC, Bridges RJ. Pharmacology of CFTR chloride channel activity. Physiol Rev 1999;79:S109–144. [PubMed: 9922378]

36. Sheppard DN, Welsh MJ. Structure and function of the CFTR chloride channel. Physiol Rev 1999;79:S23–45. [PubMed: 9922375]

37. Jentsch TJ, Stein V, Weinreich F, Zdebik AA. Molecular structure and physiological function of chloride channels. Physiol Rev 2002;82:503–568. [PubMed: 11917096]

38. Bradbury NA. Intracellular CFTR: localization and function. Physiol Rev 1999;79:S175–191. [PubMed: 9922381]

39. Riordan JR. Assembly of functional CFTR chloride channels. Annu Rev Physiol 2005;67:701–718. [PubMed: 15709975]

40. Dormer RL, McNeilly CM, Morris MR, Pereira MM, Doull IJ, Becq F, Mettey Y, Vierfond JM, McPherson MA. Localisation of wild-type and DeltaF508-CFTR in nasal epithelial cells. Pflugers Arch 2001;443(Suppl 1):S117–120. [PubMed: 11845316]

41. Yoshimura K, Nakamura H, Trapnell BC, Chu CS, Dalemans W, Pavirani A, Lecocq JP, Crystal RG. Expression of the cystic fibrosis transmembrane conductance regulator gene in cells of non-epithelial origin. Nucleic Acids Res 1991;19:5417–5423. [PubMed: 1717947]

42. Moreland JG, Davis AP, Bailey G, Nauseef WM, Lamb FS. Anion Channels, Including ClC-3, Are Required for Normal Neutrophil Oxidative Function, Phagocytosis, and Transendothelial Migration. J Biol Chem 2006;281:12277–88. [PubMed: 16522634]

43. Painter RG, Wang G. Direct measurement of free chloride concentrations in the phagolysosomes of human neutrophils. Anal Chem 2006;78:3133–3137. [PubMed: 16643004]

44. Boucher RC. New concepts of the pathogenesis of cystic fibrosis lung disease. Eur Respir J 2004;23:146–158. [PubMed: 14738247]

45. Schutte BC, McCray PB Jr. [beta]-defensins in lung host defense. Annu Rev Physiol 2002;64:709–748. [PubMed: 11826286]

46. Singh PK, Parsek MR, Greenberg EP, Welsh MJ. A component of innate immunity prevents bacterial biofilm development. Nature 2002;417:552–555. [PubMed: 12037568]

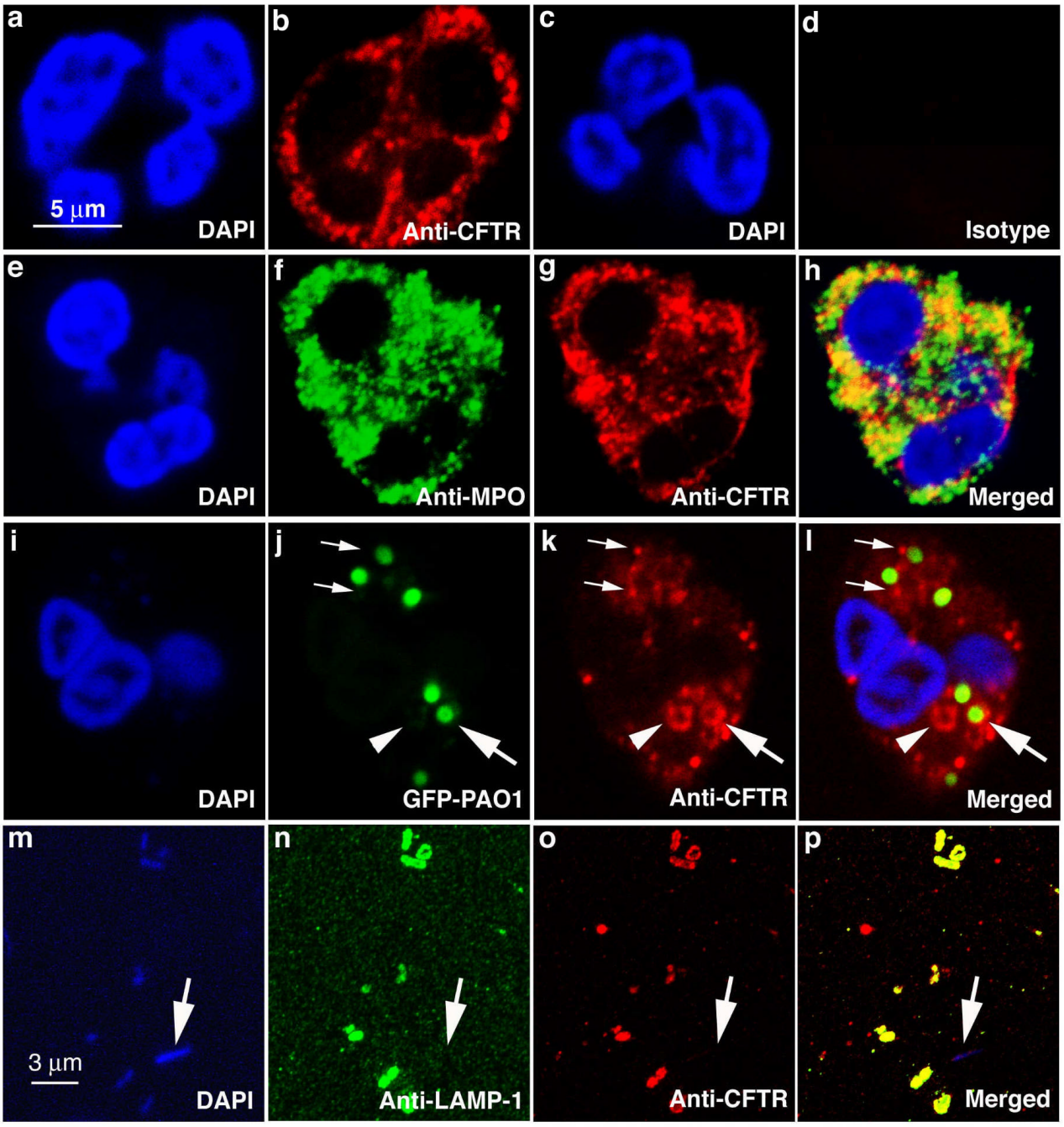

Figure 1. Localization of CFTR in human neutrophils and phagolysosomes

a & c, DAPI staining of nuclei of human neutrophils. **b**, anti-CFTR antibody staining of a human neutrophil revealing a punctate staining pattern. **d**, isotype-matched antibody staining as a control. ***e–h***, double immunofluorescent staining with rabbit anti-human myeloperoxidase antibody (**f**) and mouse anti-CFTR antibody (**g**). The merged image (**h**) to identify co-localization of CFTR and MPO. ***i–l***, CFTR association with phagocytic vacuoles and phagolysosomes bearing ingested green fluorescence protein-expressing *Pseudomonas aeruginosa* (GFP-PAO1). DAPI staining of a neutrophil with ingested bacteria (**i**). Phagocytosed GFP-PAO1 (**j**). Anti-CFTR immunofluorescent staining of a neutrophil with ingested bacteria (**k**). Association of internalized GFP-PAO1 bacteria with CFTR (**l**). Large

arrows point to a phagolysosome where CFTR is present on the membrane (**j–i**). Small arrows point to the CFTR-positive staining granules appearing attached to the phagosomes with ingested GFP-PAO1 (**j–i**). Arrowheads point to a phagocytic vacuole (**j–i**). ***m–p***, co-localization of CFTR and lysosomal associated membrane protein-1(LAMP-1) in isolated phagolysosomes. DAPI staining of phagolysosomes with ingested non-fluorescent PAO1 which are stained blue (**m**). LAMP-1 is localized to the phagolysosomes (**n**). CFTR is present in the phagolysosomal membranes (**o**). Merged image shows the co-localization of the two proteins (**p**).

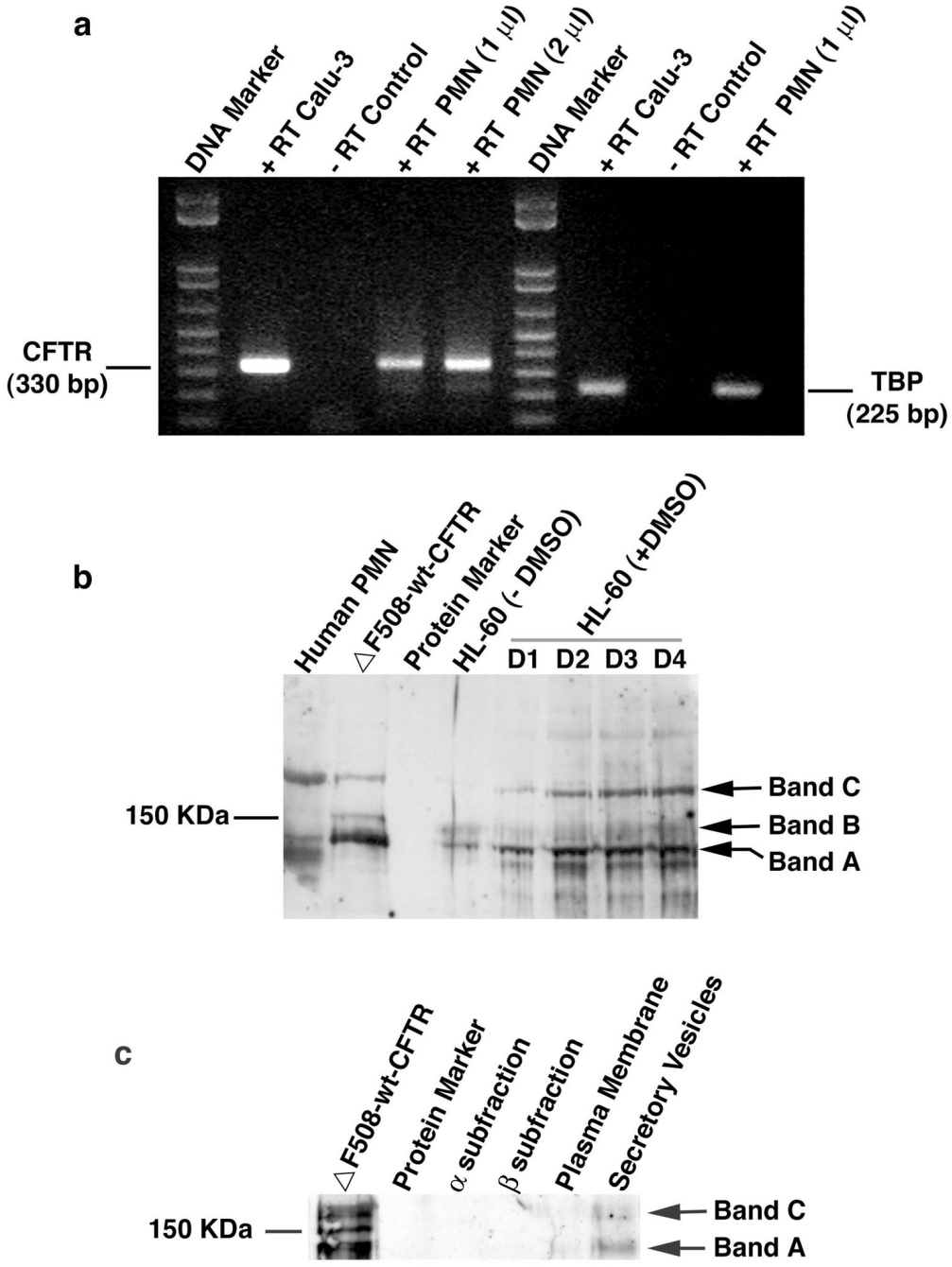

Fig. 2. CFTR expression in human neutrophils (PMN) and differentiated HL-60 cells induced by DMSO

a) RT-PCR to identify CFTR expression in human neutrophils at the mRNA level. Neutrophils were isolated from whole peripheral blood by Percoll-gradients and further purified by a panning procedure taking advantage of neutrophil adherence to plastic surface. Total RNAs were extracted and cDNAs were obtained by reverse-transcription using the CFTR and TBP specific primers. PCR amplification resulted in a CFTR amplicon of 330 bp and TBP 225 bp. Calu-3 is an epithelial cell line derived from airway submucosal gland, which is known to express high levels of CFTR. − RT or + RT represents PCR in the absence or presence of the corresponding RT product. PMN (1 μl) or PMN (2 μl) indicates PCR with 1 μl or 2 μl of PMN

RT product to show the dose-dependence of RT. **b**) Immunoblotting of CFTR of human neutrophils and differentiated HL-60 cells. Neutrophils or HL-60 cells were denatured by TCA to prevent proteolytic degradation by neutrophil-bearing proteases. 7.5% SDS-PAGE was used to resolve the proteins. After being transferred to a nitrocellulose membrane, the membrane was incubated with the CFTR-specific antibody followed by incubation with the goat anti-mouse IgG conjugated with horseradish peroxidase for chemilluminescent detection. ΔF508-wt-CFTR: wild-type CFTR gene-corrected epithelial cell line derived from a ΔF508 CF patient; HL-60: human promyelocytic leukemia cell line. Bands A, B and C represent the three forms of CFTR (Band A: newly synthesized CFTR; Band B: partially glycosylated CFTR; Band C: fully glycosylated mature CFTR). D1–4 indicates times in days after DMSO treatment. **c**) Immunoblotting of CFTR in subcellular fractions of normal human neutrophils. MPO-rich α granule fractions, vitamin B-12 binding protein-rich β granules and alkaline phosphatase-rich γ fractions were isolated. The γ fractions were further separated into secretory vesicles (SV) and plasma membrane-derived vesicles (PM) by free flow electrophoresis after treated with neuronamidase. 20–50 × 10^6 cell equivalents of α and β fractions were TCA-precipitated, and the dissolvable proteins were loaded into each lane. For SV and PM, the dissolvable proteins from ~350 × 10^6 cell equivalents of TCA-precipitated fractions were loaded, respectively. The CFTR expression in the forms of newly synthesized non-glycosylated protein (Band A) and the mature glycosylated protein (Band C) was predominantly detected in the SV fraction.

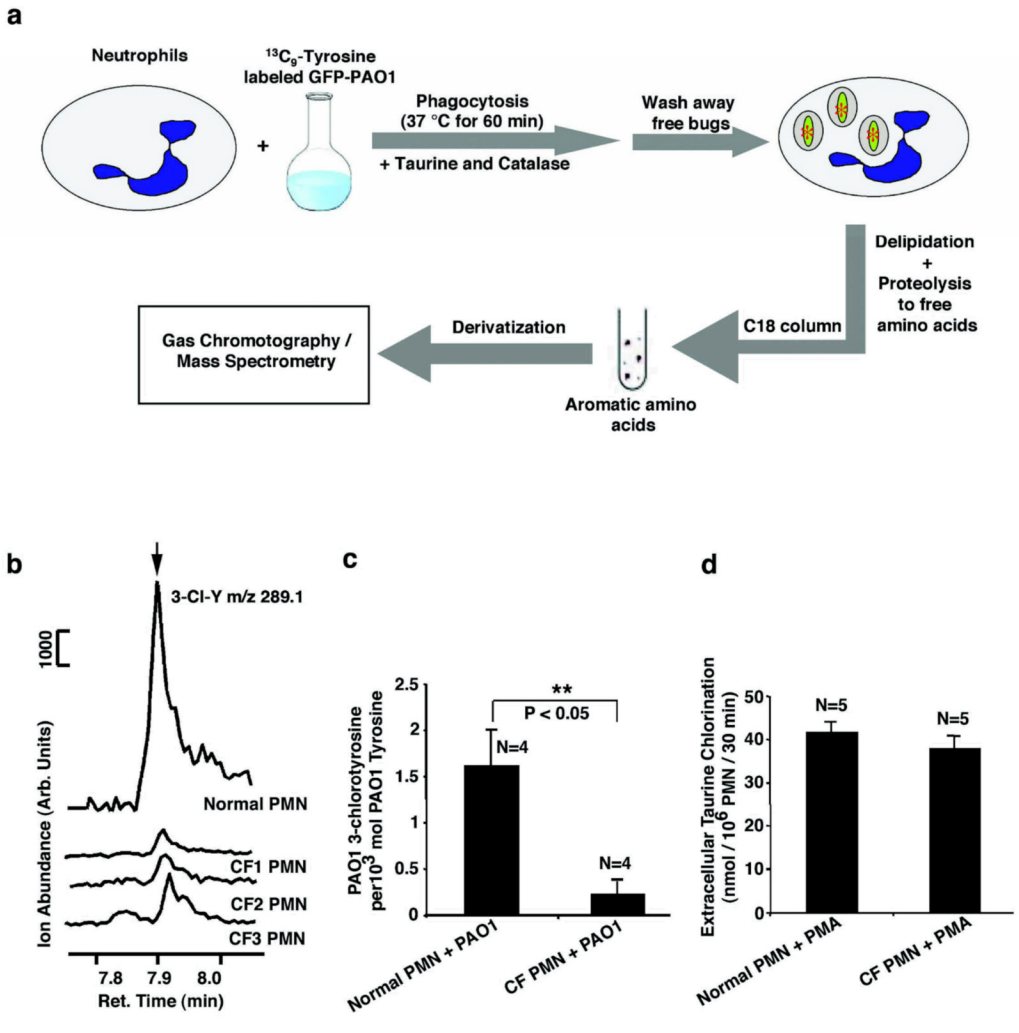

Figure 3. Intraphagolysosomal chlorination of bacterial proteins by human neutrophils from normal and CF donors

a, schematic flow diagram of the experimental protocol. Neutrophils (PMN) were incubated with green fluorescence protein-expressing *Pseudomonas aeruginosa* (GFP-PAO1) which had been metabolically prelabeled with $^{13}C_9$-L-tyrosine. After 60 min at 37° C, the uningested bacteria were removed by low speed centrifugation and the neutrophils containing ingested PAO1 were analyzed for $^{13}C_9$-3-chlorotyrosine ($^{13}C_9$-3-Cl-Y) and $^{13}C_9$-L-tyrosine ($^{13}C_9$-Y) as described in the Materials and Methods using the isotope dilution method. $^{13}C_6$-3-Cl-Y (20 pmol) and $^{13}C_6$-Y (50 nmol) were used as internal standards. After derivatization, the samples were analyzed by GC/MS using the selected ion mode. **b**, Representative GC/MS tracings obtained with normal and CF neutrophils. The 289.1 m/z peak eluting at 7.88 min, obtained by monitoring the ion at m/Z 289.1, is associated with PAO1-derived 3-chlorotyrosine. Normal neutrophils show significantly higher levels of chlorotyrosine relative to that seen from CF neutrophils. CF1, CF2, and CF3 are neutrophils (PMN) from 3 different CF donors. **c**, Ratios of PAO1-derived 3-chlorotyrosine relative to total PAO1-derived tyrosine levels after one hour of incubation with normal or CF patient neutrophils. Error bars indicate the standard error of the mean. Student's t-test proved a significant difference between normal and CF PMNs ($P<0.05$, N=4). **d,** Chlorination of extracellular taurine by HOCl generated by normal and CF neutrophils induced by phorbol-12-myristate-13-acetate (PMA). Statistically, no significant difference was seen between the two groups.

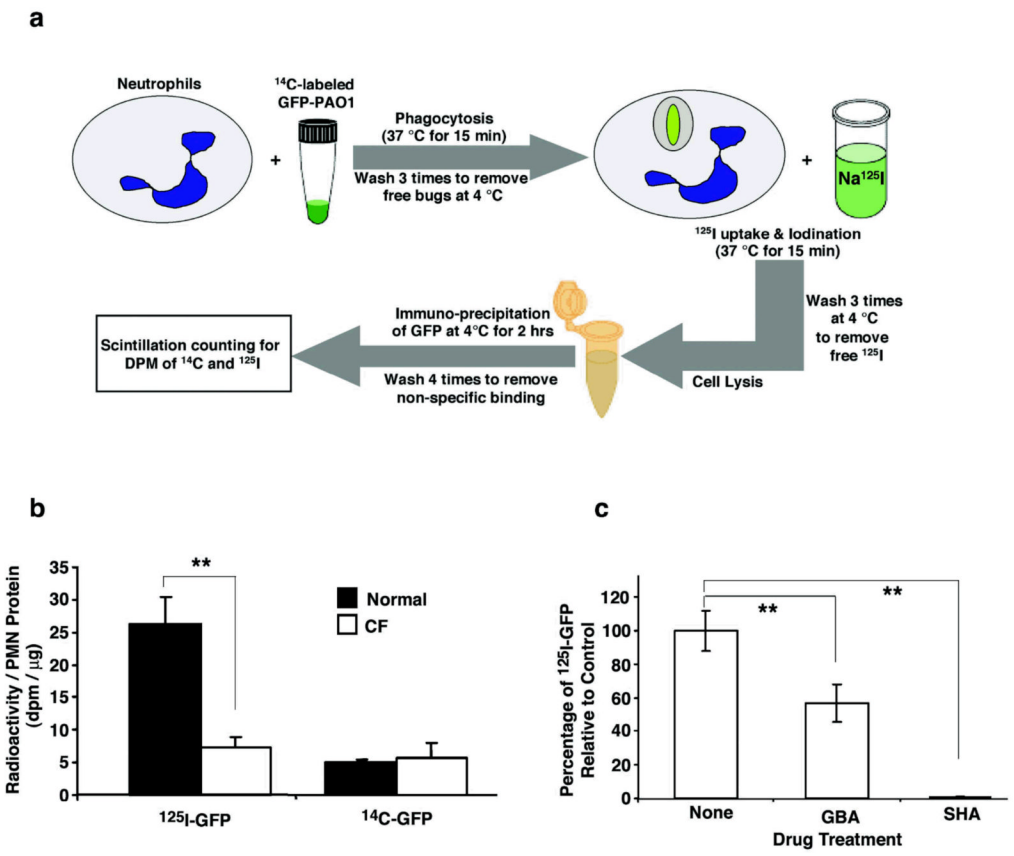

Figure 4. Intraphagolysosomal iodination of bacterial proteins by human neutrophils from normal and CF donors

a, Schematic depiction of the experimental protocol used to quantitatively measure iodination by neutrophils (PMN) of the green fluorescent protein (GFP) expressed in GFP-expressing *Pseudomonas aeruginosa*. **b,** Incorporation of ^{125}I or ^{14}C into GFP immunoprecipitated from neutrophils derived from normal donors (n= 4; *closed bars*) or donors with CF (n=4; *open bars*). The recovery of ^{14}C-GFP was similar in both normal and CF cells indicating that the amount of ^{14}C-labeled GFP-PAO1 phagocytosed by neutrophils and its subsequent recovery were statistically identical. In contrast, the ^{125}I content of recovered GFP was about 4.3-fold higher in normal neutrophils than in CF neutrophils. The error bars represent the SEM and the double asterisks represent a P value < 0.05. **c**, Glybenclamide (GBA), a CFTR channel inhibitor, significantly blocked iodination of bacteria-GFP derived from GFP-PAO1 phagocytosed by normal neutrophils as compared to controls treated with drug vehicle (None) (N=5, P<0.05). In contrast, salicylhydroxamic acid (SHA), an inhibitor of MPO, totally abolished iodination of bacteria-GFP by normal neutrophils relative to controls (N=5, P<0.01). The double asterisks indicate significant differences.